Dalton Transactions

Accepted Manuscript

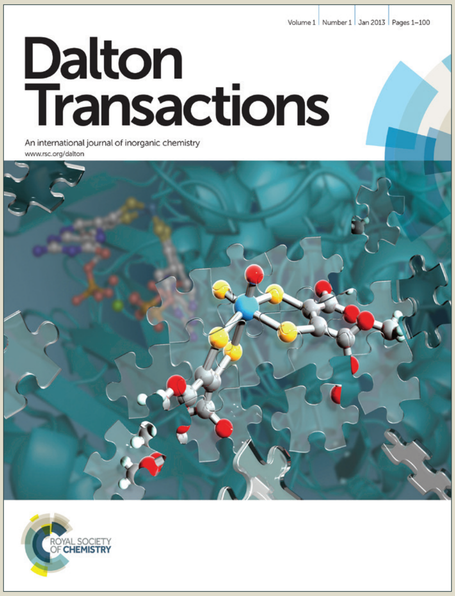

ROYAL SOCIETY OF CHEMISTRY

www.rsc.org/dalton

Cite this: DOI: 10.1039/c0xx00000x

www.rsc.org/xxxxxx

ARTICLE TYPE

Formation of self-inhibiting copper(II) nanoparticles in an autocatalytic Fenton-like reaction

Kazim R. Naqvi[a], Jennifer Marsh[b], Victor Chechik*[a]

Received (in XXX, XXX) Xth XXXXXXXXX 20XX, Accepted Xth XXXXXXXXX 20XX

DOI: 10.1039/b000000x

ABSTRACT: Cu(II)-catalysed decomposition of hydrogen peroxide at alkaline pH in the presence of etidronic acid (HEDP) showed a sigmoid kinetic profile typical of autocatalytic reactions. However, the reaction abruptly stopped well before all hydrogen peroxide had decomposed, and further addition of Cu(II) and HEDP did not restart the reaction. Results of a mechanistic study suggest that the reaction involves the formation of an active catalyst which decomposes hydrogen peroxide and oxidizes HEDP. Once all HEDP has been consumed, the active complex triggers Cu(II) aggregation to form remarkably stable but catalytically inactive nanoparticles. The nanoparticles were found to be basic Cu(II) phosphate/carbonate. They exhibit self-poisoning behaviour in the hydrogen peroxide decomposition and undergo seed-mediated growth upon addition of further Cu(II).

Introduction

Transition metal ions such as iron decompose hydrogen peroxide via a well-studied Fenton-like reaction.[1-5] This chemistry plays an important role in a range of chemical and biological environments. The most common applications of Fenton chemistry are in wastewater treatment,[6, 7] however reaction of hydrogen peroxide with metal complexes also has implications in biology and medicine, *e.g.,* in controlling production of reactive oxygen species, and involvement in many pathological processes.[8] Understanding mechanistic pathways of Fenton-like reactions is thus essential for the rational design of their applications in industrial and medicinal chemistry. Unfortunately, mechanistic details proved elusive, and the mechanism of Fenton-like reactions became the subject of debate over several decades. Formation of hydroxyl radical and/or higher oxidation state metal ion intermediates has been proposed.[9-11] Gradually, it became clear that whatever the mechanism, a number of reactive metal complexes are formed during Fenton-like reactions. The complex reaction kinetics and inherently short lifetime of the intermediate metal complexes hampered mechanistic studies. Moreover, the precise nature of reactive species appears to depend strongly on reaction conditions. In some cases, however, intermediate metal complexes formed in Fenton-like reactions have been characterized. Mononuclear peroxo or dinuclear iron oxo-bridged complexes were proposed as initial intermediates.[12, 13] For instance, reaction containing iron(III)-ethylenediaminetetraacetic acid (EDTA) gives a purple coloured peroxo complex with alkaline hydrogen peroxide.[14-16]

Just like iron, copper ions also decompose hydrogen peroxide in a reaction which has great technological and biological significance; however the mechanism of this reaction is equally complex. Initial copper concentration, the presence of ligand and/or organic substrate, pH of the reaction solution and composition of buffer greatly influence the kinetics and mechanism of hydrogen peroxide decomposition.[17, 18] Structural characterization of the intermediate complexes proved challenging; however studies in a related field of copper-dioxygen complexes revealed a wide range of structures including both mono- and dinuclear species.[19] For instance, formation of a relatively stable dicopper-peroxide intermediate (probably peroxo-bridged complex) during decomposition of hydrogen peroxide by a tridentate pyridine based Cu(II) complex has been reported.[20]

In the context of apparently large variety of mechanistic pathways and reactive intermediates in metal-catalysed decomposition of hydrogen peroxide, we noticed unusual behaviour of this reaction in the copper–etidronic acid (HEDP) ligand system in alkaline solutions. We found that copper-HEDP catalysed reaction exhibited self-accelerated, rapid initial hydrogen peroxide decomposition that terminated abruptly long before completion (Scheme 1).

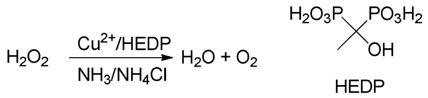

Scheme 1: Cu(II)/HEDP catalysed H_2O_2 decomposition

We were interested in this system as HEDP ligand is often employed in stabilizing hydrogen peroxide and has been used in

---

[a] *Department of Chemistry, University of York, York YO10 5DD, UK Email: victor.chechik@york.ac.uk*

[b] *The Procter and Gamble Company, Mason Business Center, 8700 Mason-Montgomery Road, Mason, Ohio 45040, USA.*

† Electronic Supplementary Information (ESI) available: experimental details, additional spectroscopic and kinetic data, metal speciation plots. See DOI: 10.1039/b000000x/

oxidative hair colouring formulations to prevent its decomposition.[21] While there are many reports of copper involving Fenton chemistry under acidic conditions, very little information is available for the alkaline system. The focus of this study was therefore to uncover the roots of the self-inhibiting behaviour in the autocatalytic Cu-HEDP system at high pH. We did not determine the structure of the active catalyst; this is a very challenging task well beyond the scope of the present study. However, we felt that obtaining general mechanistic understanding would not only broaden the scope of our understanding of the Fenton-like reactions but would also be relevant to the industrial chemistry.

Results and discussion

Fenton reaction with Cu-HEDP at pH 10

In our reactions, copper(II) sulfate (4.5 µmol), HEDP ligand (32.5 µmol) and hydrogen peroxide (24.5 mmol) were mixed with 20 mM pH 10 ammonia/ammonium chloride buffer (total reaction volume 25 mL). The profile for oxygen evolution during the decomposition reaction showed a sigmoid trend typical of an auto-catalytic reaction. However, only a small amount of oxygen evolved and no further oxygen evolution was observed after 16-18 min of the reaction (Figure 1, curves B). Substantial quantity of hydrogen peroxide was still present at the end of decomposition, as shown by the addition of catalase which led to further peroxide decomposition and oxygen evolution.

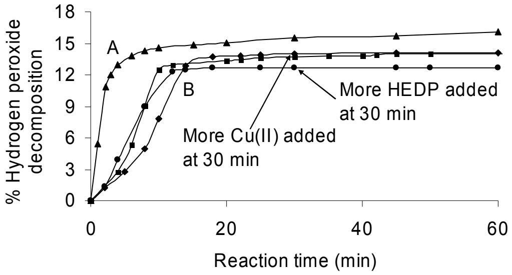

Figure 1: Cu(II)-catalysed decomposition of alkaline hydrogen peroxide in the presence of HEDP (32.5 µmol) with 20 mM pH 10 ammonia/ammonium chloride buffer: (A) 20 µmol Cu^{2+} (triangles); (B) 4.5 µmol Cu^{2+} (squares). The experiments shown with diamonds and circles were also run with 4.5 µmol Cu^{2+}; but these experiments had additional 4.5 µmol Cu^{2+} or 32.5 µmol of HEDP added to the reaction mixture 30 min after the start of the reaction (as indicated by the arrows). The standard mean error for the determination of hydrogen peroxide decomposition here and in all following experiments was 0.5 %

Increasing Cu(II) concentration increased the rate of reaction (Figure 1, curve A), while increased ligand concentration slowed the reaction down (Figure 2, curve B). However, the overall shape of the kinetic profile was not affected. In the absence of HEDP ligand (Figure 2, curve C) or in the presence of other ligands (vide infra), the sigmoidal kinetic profile was not observed. Changes in pH and the concentration of base strongly influenced the reaction kinetics. Reaction proceeded rapidly to completion at high ammonia concentration (e.g., in 400 mM ammonium buffer) (Figure 2, curve F). This is not unexpected as Cu(II) speciation in the reaction mixture would strongly depend on pH and ammonia concentration (vide infra).

The abrupt termination of the catalytic decomposition could be caused by either degradation of the catalyst, or formation of a self-poisoning species. Surprisingly, addition of either fresh copper (II) ions or HEDP ligand did not restart peroxide decomposition (Figure 1, curves B shown with diamonds and circles, respectively). We therefore argued that catalyst degradation alone cannot be responsible for the premature reaction end, and some sort of self-inhibiting products must be formed. In order to determine the structure of these reaction products, we analysed the composition of the reaction mixture at the end of hydrogen peroxide decomposition.

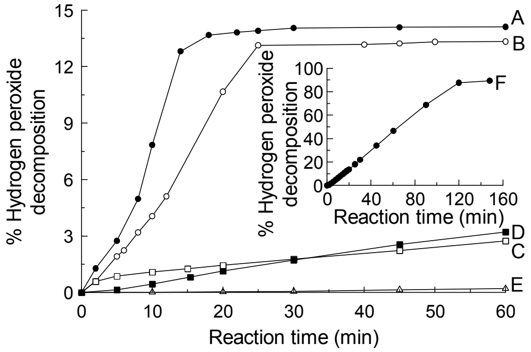

Figure 2: Decomposition of hydrogen peroxide in Cu(II)-HEDP reaction system with pH 10 ammonia/ammonium chloride buffer. Unless stated otherwise, the amounts/concentrations are as follows: 4.5 µmol Cu^{2+}, 32.5 µmol HEDP ligand, 20 mM ammonia/ammonium chloride buffer.(A) benchmark reaction, (B) 65 µmol HEDP ligand, (C) without ligand, (D) in 20 mM pH 9 ammonia/ammonium chloride buffer, (E) in 20 mM pH 8 ammonia/ammonium chloride buffer, (F) in 400 mM pH 10 ammonia/ammonium chloride buffer

HEDP ligand degradation

As the reaction was found to be strongly pH-sensitive, we first monitored the pH changes during hydrogen peroxide decomposition. We noticed that pH of the reaction mixture changed from 10.0 to 9.18 upon mixing the reagents. This is consistent with the value calculated by taking into account pK_a of hydrogen peroxide and HEDP. The pH of the reaction solution however continued to drop during the course of decomposition and only stabilized when the oxygen evolution stopped. Overall, pH dropped from 9.18 to 8.92 (Figure 3A). No further pH drop was observed afterwards. This small change of pH, however, cannot account for the abrupt end of the reaction. When the initial pH of reaction mixture was 9.55, it dropped during reaction to 9.33, but the reaction profile was essentially identical to that of the reaction with initial pH of 9.18, and decomposition of hydrogen peroxide stopped abruptly after 16-18 min. Increasing pH after the end of either reaction mixture also did not restart hydrogen peroxide decomposition.

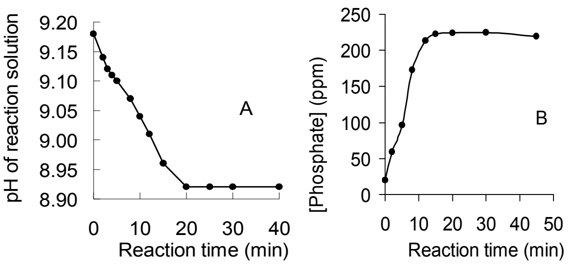

Figure 3: (A) pH drop and (B) phosphate evolution during the course of hydrogen peroxide decomposition. The standard mean error for pH and phosphate measurements was 0.01 and 15 ppm, respectively.

The pH drop during the reaction is unexpected as the decomposition of slightly acidic hydrogen peroxide should lead to the increased pH. The observed pH change can be explained by oxidation of either ammonia or HEDP ligand to acidic products. Ammonia in the strongly oxidising Fenton-like system would be expected to produce nitric acid. However, nitrate analysis by ion exchange chromatography gave negative result. On the other hand, the pH drop was quantitatively explained by complete oxidation of the HEDP ligand to form phosphate and carbonate ions. Degradation of organic substrates in a Fenton-like reaction has been reported in literature.[22, 23] For instance, aminocarboxylate ligands such as EDTA and ethylenediamine-N,N'-disuccinic acid (EDDS) are prone to complete degradation *via* a radical mediated mechanism.[15, 24] Organic phosphates and phosphonates have also been reported to undergo degradation.[25, 26] The phosphate analysis of the reaction mixture showed immediate release of phosphate ion on mixing with hydrogen peroxide. This suggests an immediate start of ligand degradation. The phosphate release profile (Figure 3B) closely mirrored that for the oxygen evolution, with the concentration increasing over time until hydrogen peroxide decomposition stopped. To explain the pH drop quantitatively, complete ligand degradation at the end of reaction must be assumed. Thus is consistent with the ^{1}H and ^{13}P NMR results which showed no HEDP signals in the reaction product. In summary, hydrogen peroxide decomposition in Cu(II)-HEDP system is accompanied by HEDP degradation to carbonate and phosphate. Complete degradation of HEDP coincides with the abrupt end of the peroxide decomposition.

Formation of copper based nanoparticles

We noticed that the reaction solution suddenly became brown coloured at the end of the reaction. The UV-Vis analysis of the reaction mixture at the end of decomposition revealed a broad featureless spectrum (Figure 4A). This absorption is typical of inorganic nanoparticles. For instance, ligand-protected copper(II) oxide nanoparticles show similar UV spectra and hence similar colour.[27, 28] TEM images confirmed formation of small nanoparticles (average diameter 3.0±1.0 nm, Figure 4B). The nanoparticles can be purified by dialysis against water. Interestingly, the nanoparticles showed remarkable stability as no aggregation was observed upon storage in solution for 4 weeks at room temperature.

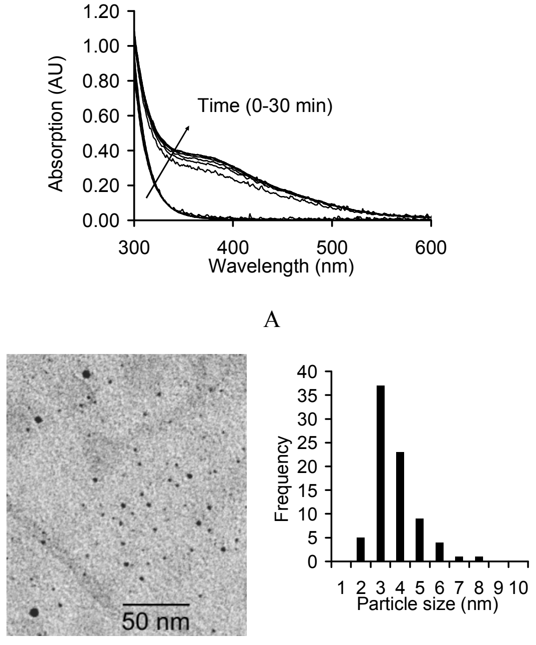

B

Figure 4: (A) UV-Vis spectra of Cu(II)-HEDP reaction solution recorded over time showing absorption band for copper nanoparticles; (B) TEM image and size distribution of copper nanoparticles in Cu-HEDP reaction mixture.

To establish the chemical composition of nanoparticles, they were isolated, purified by dialysis and characterized. The elemental composition of nanoparticles showed the presence of carbon (1.53%) along with hydrogen (1.25%). ICP-OES results gave copper (53.5%) and phosphorus (5.35%) content (Figure S1). The C/H ratio is inconsistent with HEDP ligand. The ^{1}H and ^{31}P NMR of acid-degraded nanoparticles also did not show any signal for HEDP ligand (Figure S2).

As we observed formation of inorganic phosphate in the reaction mixture at the end of decomposition, we speculated that the presence of C and P can be due to the carbonate and phosphate. Phosphate analysis of the acid-degraded nanoparticles indeed confirmed the presence of phosphate at significant level (13±1) %. The presence of carbonate ions in the nanoparticles was confirmed by analyzing the IR spectrum of carbon dioxide gas evolved on dissolving these nanoparticles in a strong acid (Figure S3). A quantitative analysis gave (7.7±0.2) % of carbonate content in the nanoparticles. The data from elemental analysis, ICP-OES, phosphate and carbonate analysis were modelled together to obtain the nanoparticle composition. The results suggest that the nanoparticles are a mixture of basic copper phosphate and carbonate. The nanoparticles also contained ca. 6% of strongly adsorbed water that cannot be removed by keeping the nanoparticles under vacuum (Table 1).

Compound	w/w %
$Cu_2(OH)_2CO_3$	34
$Cu_3(OH)_3PO_4$	60
H_2O	6

Table 1: Chemical composition of Cu(II) nanoparticles isolated from Cu(II)-HEDP catalyzed decomposition of alkaline hydrogen peroxide.

The oxidations state of copper in the nanoparticles can conceivably be 0, +1, +2 or +3. Formation of copper metal in the strongly oxidising medium is highly unlikely, and is inconsistent with the results of elemental analysis. In order to confirm the oxidation state of copper in the nanoparticles, they were dissolved in concentrated hydrochloric acid under inert atmosphere. UV-Vis spectra of the resultant solution showed quantitative formation of Cu(II) chloride ($CuCl_4^{2-}$). As UV spectra clearly differentiate Cu(I) and Cu(II) chlorides, this experiment makes it possible to rule out Cu(I) as the nanoparticle constituent. Formation of Cu(III) species in Fenton-like reaction would be a tantalising possibility, and we note that some Cu(III) compounds have UV-Vis spectra similar to that recorded for the nanoparticles.[29] However, most Cu(III) compounds are very unstable[30] and while Cu(III) could be an intermediate in the reaction, it is highly unlikely to form very stable nanoparticles as the reaction product. In addition, Cu(III) nanoparticles are inconsistent with the elemental analysis. All these arguments are consistent with the nanoparticle composition given in Table 1

Formation of basic copper(II) phosphate/carbonate is in reasonable agreement with the copper speciation plots calculated for the experimental conditions using Medusa software[31] (Figure S4, S5) and literature binding constants.[32] The accuracy of the data for copper phosphate is uncertain, and in any case the binding constants will be strongly affected by the nanoscopic size of the particles. Nonetheless, speciation plots clearly suggest formation of basic copper phosphate under reaction conditions.

Variation of reaction conditions also leads to results consistent with the speciation plots. Adding phosphate and carbonate to an ongoing hydrogen peroxide decomposition reaction mixture does not change the overall reaction profile (Figure S6). Carrying out the reaction in a 20 mM phosphate buffer slows the reaction down but also does not change the decomposition profile (Figure S7). Increase in ammonia concentration to 400 mM prevents nanoparticle formation and leads to very fast hydrogen peroxide decomposition, consistent with the generation of highly active copper-ammonia complex as predicted by the speciation modelling (Figures S8-S9).

Pathway for the formation of nanoparticles

On the basis of the above observations, we can explain the course of the reaction (Scheme 2). The reaction involves formation of a highly reactive intermediate, probably an HEDP-containing oxo- or peroxy bridged copper complex. Formation of di, tri- and multinuclear copper-oxo bridged species has been proposed and observed previously.[33-35] In particular, several multinuclear copped-HEDP complexes have been reported in the literature[36, 37] These layered materials, prepared by a hydrothermal method, have phosphate and oxo bridges as revealed from the XRD data.

Formation of an active complex in our system explains the sigmoid profile of the reaction kinetics. The reactive intermediates lead not only to hydrogen peroxide decomposition, but also HEDP degradation. Monomeric and dimeric copper oxygen complexes have been reported to possess high catalytic activity for oxidizing organic molecules with hydrogen peroxide.[19, 38-42] Once all HEDP ligand has been degraded, the HEDP-free copper intermediates act as seeds to nucleate formation of basic copper phosphate/carbonate nanoparticles which have no catalytic activity. Nanoparticle formation is irreversible; hence addition of more HEDP ligand at the end of reaction does not result in further decomposition of hydrogen peroxide. In order to test the proposed pathway, we carried out additional experiments.

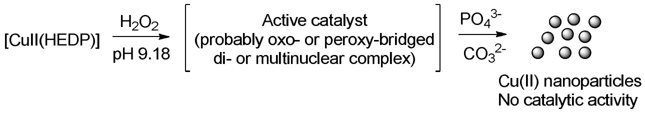

Scheme 2: Proposed pathway for the formation of copper nanoparticles in Cu(II)-HEDP catalysed decomposition of alkaline hydrogen peroxide.

Role of hydrogen peroxide

Upon inspection of speciation plots (Figure S4), one should notice that Cu(II) oxide is the predominant species formed under reaction conditions. Copper(II)-based nanoparticles would therefore be expected to form even in the absence of hydrogen peroxide. However we observed no nanoparticle formation in the absence of hydrogen peroxide under these conditions, even in the presence of HEDP and/or phosphate/carbonate ions. The formation of copper(II) oxide is presumably limited by kinetic factors. We therefore hypothesise that the role of hydrogen peroxide in the nanoparticle formation is to generate an active catalyst, probably an oxo- or peroxy-bridged complex which upon oxidation of the stabilising ligand (HEDP) acts as a seed for the nanoparticle formation thus overcoming the kinetic barrier to nucleation. This unusual role of hydrogen peroxide in nanoparticle nucleation is consistent with the proposed mechanism and experimental observations.

By carefully varying the reaction conditions, we were able to form copper phosphate/carbonate nanoparticles in the absence of hydrogen peroxide with the properties nearly identical to those of the nanoparticles formed in peroxide decomposition reaction; however this required much higher temperature and long reaction time (Figures S13-S15). Nonetheless, this experiment further supports the proposed composition of the nanoparticles.

Self-inhibiting behaviour of Cu(II) nanoparticles

As the copper phosphate/carbonate nanoparticles are the main product of the reaction, they must possess self-inhibiting properties observed in the overall process. This can be understood if we assume that nanoparticle surface provides seeds for further nanoparticle growth upon addition of extra Cu(II) at the end of reaction. Any added Cu(II) ions get immediately adsorbed on the nanoparticle surface. Therefore, no reactive intermediates are formed and the hydrogen peroxide decomposition is not observed.

In order to test this hypothesis, we carried out a series of control experiments. Variable amounts of fresh Cu(II) sulfate were added to the nanoparticle solution at the end of hydrogen peroxide decomposition and the reaction mixtures were examined using UV-Vis spectroscopy. Instant and almost linear increase in the absorption was consistent with the nanoparticle growth (Figure 5). The nanoparticle solution remained stable and no precipitation was observed until Cu(II) concentration reached 0.8 mM, at which point a brown precipitate was found. Thus, the experimentally observed inability of freshly added Cu(II) to restart the hydrogen peroxide decomposition can be attributed to the rapid adsorption of Cu(II) on the nanoparticle surface leading to the growth of catalytically inactive particles and thus self-poisoning.

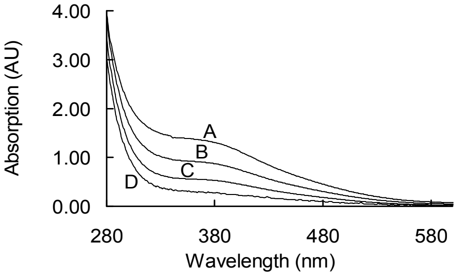

Figure 5: Fresh addition of Cu(II) sulfate to the nanoparticle solution in pH 10 ammonia/ammonium chloride buffer leads to an increased UV-Vis absorption. Amount of Cu^{2+} added: (A) 19 µmol; (B) 13.5 µmol; (C) 9 µmol; (D) 4.5 µmol.

The observed effect of changing the metal to ligand ratio on the kinetic profile of the decomposition reaction (Figures 1-2) can now be explained in terms of the proposed reaction pathway. Increased Cu(II) concentration leads to a faster hydrogen peroxide decomposition (presumably due to the higher concentration of the active catalyst) and also to a faster nanoparticle formation (due to faster nucleation/growth). Increased concentration of HEDP stabilizes the initial complex and hence slows down the formation of the active catalyst and decreases the rate of hydrogen peroxide decomposition (Figure 2).

Defeating the self-inhibiting effect: the role of HEDP ligand

In the proposed reaction mechanism, the nanoparticle nucleation only occurs after complete degradation of HEDP which presumably is involved in the structure of the active catalyst. This conclusion makes it possible to rationally design reaction conditions that would not exhibit self-poisoning effect. Continuous addition of HEDP ligand to an ongoing hydrogen peroxide decomposition reaction should prevent the active catalyst from nucleating the nanoparticles. In a control experiment, we added HEDP in three batches at different reaction times before the nanoparticle formation was observed. As HEDP decomposition gives acidic products and hence leads to pH drop, we re-adjusted the pH with NaOH half way through the reaction to maintain the reaction conditions unchanged. This simple procedure indeed prevented the nanoparticle formation and induced continuous decomposition of hydrogen peroxide with no sign of self-inhibition (Figure 6). This experiment strongly suggests that the trigger for nanoparticle nucleation is complete oxidation of HEDP which is consistent with the proposed mechanism.

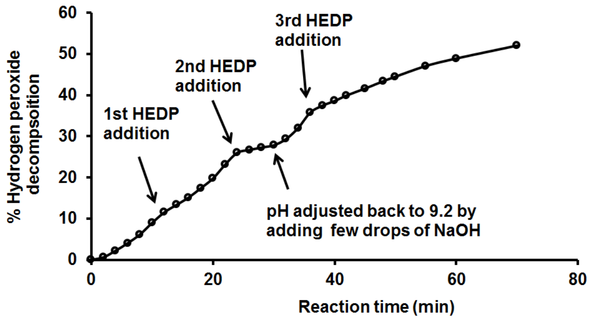

Figure 6: Adding fresh HEDP ligand to an ongoing Cu(II)-HEDP catalysed hydrogen peroxide decomposition reaction just before it stops. Pre-neutralised HEDP (32.5 µmol each time) ligand was added at different time intervals. pH of the reaction solution was maintained by adding a few drops of 2M sodium hydroxide.

The nature of the active catalyst

Unfortunately, our attempts to characterize the active intermediate were unsuccessful. EPR spectra of reaction solutions crash-frozen at different time intervals showed complex pattern due to the presence of several Cu(II) species (consistent with the speciation predictions) but neither the lineshape nor the intensity changed up until the end of hydrogen peroxide decomposition, at which point EPR signal abruptly disappeared, consistent with the nanoparticle formation. (Figure 7). Mass spectroscopic (ESI) investigation did not show any new Cu(II) complexes. UV-Vis spectra showed some small changes in the lineshape consistent with the changes in the copper speciation during the course of hydrogen peroxide decomposition (Figure S16). Taken together, these data suggest that the concentration of the active catalyst is very low throughout the reaction, and complete degradation of HEDP ligand triggers very fast nucleation and growth of the nanoparticles.

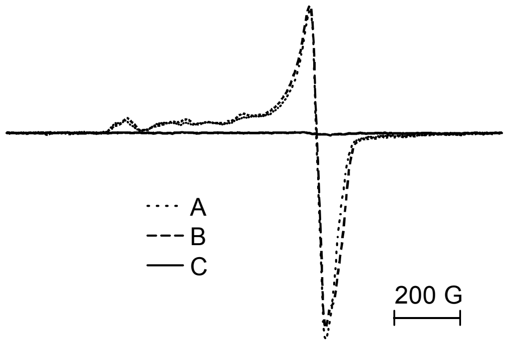

Figure 7: EPR spectra of copper-HEDP reaction solution. Reaction solution contained Cu^{2+} (4.5 µmol), HEDP (32.5 µmol) in 20 mM pH 10 ammonia/ammonium chloride buffer with hydrogen peroxide (24.5 mmol), total reaction volume 25 mL. Aliquots (1.6 mL) were mixed with glycerol (0.4 mL) in a quartz EPR tube, and spectra were recorded at 120 K at the following times after the start of the reaction: (A) 2 min; (B) 8 min; (C) 15 min.

Despite the failure to characterise the active catalyst, it is clear that the HEDP ligand is essential for its generation. No nanoparticle formation was observed when the reactions were repeated in the presence of other ligands [EDTA, ethylenediamine-N,N'-disuccinic acid (EDDS), diethylenetriamine penta(methylene phosphonic acid (DTPMP), diethylenetriamine pentaacetic acid (DTPA)], phosphate ion, and in the absence of any ligand. One can hypothesise that strongly coordinating hexa- and octadentate ligands do not favour formation of bridged copper dimers/oligomers which are likely to be the active species in the hydrogen peroxide decomposition reaction.

The reaction in a ligand-free system in an ammonia buffer (Figure 2) showed immediate nanoparticle formation upon addition of hydrogen peroxide as evidenced by the UV spectra; however these materials were unstable and quickly precipitated from solution (Figure S17). Carrying out reaction in a ligand-free 20 mM phosphate buffer also resulted in the immediate formation of somewhat more stable nanoparticles which showed very little catalytic activity (Figure S18). The presence of phosphate thus seems critical for the formation of stable nanoparticles.

Conclusions

In summary, we found that the decomposition of hydrogen peroxide by Cu(II)-HEDP mixture at alkaline pH proceeds via formation of an active catalyst that degrades the ligand and eventually seeds formation of catalytically-inactive basic copper phosphate/carbonate nanoparticles. The nanoparticles prevent any further catalytic reaction as freshly added Cu(II) ions quickly adsorb on their surface and do not form active catalyst. This is a rather unusual scenario for the Fenton-like chemistry; however it is perhaps not so uncommon in other areas. For instance, many Pd-catalysed cross-coupling reactions proceed via formation of an active catalyst. There is evidence that at least in some cases multinuclear clusters possess high catalytic activity. At the end of the reaction, the active catalyst nucleates formation of bigger particles which eventually precipitate to form Pd black which is usually catalytically inactive. The lability of the active catalyst in this type of reaction is essential for the high catalytic activity; yet it facilitates eventual nucleation to form inactive larger particles. We believe Cu-HEDP catalyzed degradation of hydrogen peroxide follows the same principles.

Acknowledgments

The authors would like to thank the Procter and Gamble Company and Wild Fund (University of York) for funding this work.

References

1. H. Fenton, *J. Chem. Soc., Trans.*, 1894, **65**, 899 - 910.
2. P. Wardman and L. P. Candeias, *Radiat. Res.*, 1996, **145**, 523-531.
3. W. H. Koppenol, *Free Radical Biol. Med.*, 1993, **15**, 645-651.
4. S. Goldstein, D. Meyerstein and G. Czapski, *Free Radical Biol. Med.*, 1993, **15**, 435-445.
5. G. Chen, *Angew. Chem. Int. Ed.*, 2010, **49**, 5413-5415.
6. L. Gomathi Devi, S. Girish Kumar, K. Mohan Reddy and C. Munikrishnappa, *J. Hazard. Mater.*, 2009, **164**, 459-467.
7. L. G. Devi, K. S. A. Raju and S. G. Kumar, *J. Environ. Monit.*, 2009, **11**, 1397-1404.
8. J. Prousek, *Pure Appl. Chem.*, 2007, **79**, 2325-2338.
9. W. Freinbichler, K. F. Tipton, L. Della Corte and W. Linert, *J. Inorg. Biochem.*, 2009, **103**, 28-34.
10. S. Rachmilovich-Calis, A. Masarwa, N. Meyerstein, D. Meyerstein and R. van Eldik, *Chem. Eur. J.*, 2009, **15**, 8303-8309.
11. W. H. Koppenol, *J. free radic. biol. med.*, 1985, **1**, 281-286.
12. A. Brausam and R. van Eldik, *Inorg. Chem.*, 2004, **43**, 5351-5359.
13. L. Westerheide, F. K. Muller, R. Than, B. Krebs, J. Dietrich and S. Schindler, *Inorg. Chem.*, 2001, **40**, 1951-1961.
14. C. Walling, R. E. Partch and T. Weil, *Proc. Natl. Acad. Sci. USA*, 1975, **72**, 140-142.
15. C. Walling, M. Kurz and H. J. Schugar, *Inorg. Chem.*, 1970, **9**, 931-937.
16. K. C. Francis, D. Cummins and J. Oakes, *J. Chem. Soc., Dalton Trans*, 1985, 493-501.
17. J. F. Perez-Benito, *Mon. Chem.*, 2001, **132**, 1477-1492.
18. S. Skounas, C. Methenitis, G. Pneumatikakis and M. Morcellet, *Bioinorg. Chem. Appl.*, 2010.
19. L. M. Mirica, X. Ottenwaelder and T. D. P. Stack, *Chem. Rev.*, 2004, **104**, 1013-1046.
20. Q. Zhu, Y. Lian, S. Thyagarajan, S. E. Rokita, K. D. Karlin and N. V. Blough, *J. Am. Chem. Soc.*, 2008, **130**, 6304-6305.
21. C. Zavik and J. Milliquent, in *The Science of Hair Care*, eds. C. Bouillon and J. Wilkison, Taylor & Francis Group, LLC London, 2nd edn., 2005, pp. 246-268.
22. M. E. T. Sillanpää, T. Agustiono Kurniawan and W.-h. Lo, *Chemosphere*, 2011, **83**, 1443-1460.
23. A. Masarwa, S. Rachmilovich-Calis, N. Meyerstein and D. Meyerstein, *Coord. Chem. Rev.*, 2005, **249**, 1937-1943.
24. B. Hobel and C. von Sonntag, *J. Chem. Soc., Perkin Trans. 2*, 1998, 509-514.
25. B. Balci, M. A. Oturan, N. Oturan and I. Sirés, *J. Agric. Food Chem.*, 2009, **57**, 4888-4894.
26. K. A. Barrett and M. B. McBride, *Environ. Sci. Technol.*, 2005, **39**, 9223-9228.
27. D. R. Clary and G. Mills, *J. Phys. Chem. C*, 2011, **115**, 1767-1775.
28. A. Kumar, A. Saxena, A. De, R. Shankar and S. Mozumdar, *RSC Advances*, 2013, **3**, 5015-5021.
29. D. Meyerstein, *Inorg. Chem.*, 1971, **10**, 2244-2249.
30. A. Casitas and X. Ribas, *Chem. Sci.*, 2013, **4**, 2301-2318.
31. I. Puigdomenech, *Medusa, Chemical Equilibrium Diagrams* (2010), Stockholm.
32. A. E. Martell and R. D. Hancock, *Metal complexes in aqueous solutions*, Plenum Press, New York, 1996.
33. M. H. Robbins and R. S. Drago, *J. Catal.*, 1997, **170**, 295-303.
34. T. Osako, K. Ohkubo, M. Taki, Y. Tachi, S. Fukuzumi and S. Itoh, *J. Am. Chem. Soc.*, 2003, **125**, 11027-11033.
35. T. Osako, S. Nagatomo, T. Kitagawa, C. Cramer and S. Itoh, *J. Biol. Inorg. Chem.*, 2005, **10**, 581-590.
36. C. W. Jones, *Applications of Hydrogen Peroxide and Derivatives*, Royal Society of Chemistry, 1999.
37. L.-M. Zheng, H.-H. Song, C.-Y. Duan and Xin, *Inorg. Chem.*, 1999, **38**, 5061-5066.
38. D. Maiti, J. S. Woertink, A. A. N. Sarjeant, E. I. Solomon and K. D. Karlin, *Inorg. Chem.*, 2008, **47**, 3787-3800.

39. K. D. Karlin, C. X. Zhang, A. L. Rheingold, B. Galliker, S. Kaderli and A. D. Zuberbühler, *Inorg. Chim. Acta.*, 2012, **389**, 138-150.
40. E. I. Solomon, J. W. Ginsbach, D. E. Heppner, M. T. Kieber-Emmons, C. H. Kjaergaard, P. J. Smeets, L. Tian and J. S. Woertink, *Faraday Discuss.*, 2011, **148**, 11-39.
41. E. A. Lewis and W. B. Tolman, *Chem. Rev.*, 2004, **104**, 1047-1076.
42. A. M. Kirillov, M. N. Kopylovich, M. V. Kirillova, M. Haukka, M. da Silva and A. J. L. Pombeiro, *Angew. Chem.-Int. Edit.*, 2005, **44**, 4345-4349.

Autocatalytic Fenton-like decomposition of hydrogen peroxide in the presence of Cu(II) and etidronic acid (HEDP) at high pH results in the nucleation of very stable mixed copper(II) phosphate/carbonate nanoparticles which self-inhibit further reaction.